Analysis of density variation for different temperatures in thermal nano imprinting process

Dong Eon Lee, Hee Jung Lee, Seung Woong Choi, and Woo Il Lee

* *School of Mechanical and Aerospace Engineering, Seoul National University, Seoul 151-742, Korea, leditt79@snu.ac.kr*

ABSTRACT

The density variation of polymer resist for different temperatures in a thermal nano imprinting process [1], [2] was studied through both experimentation and molecular dynamics (MD) simulations. After patterning, we estimated the local density by measuring the pull-off force between the tip and the patterned surface using an atomic force microscope (AFM) in liquid.

Both in the results of experiment and the simulation, the density of the bottom (the pressed region of the pattern) is higher than that of the top region (the cavity region). The density difference between the top and the bottom regions was found to decrease as the processing temperature increased.

Keywords: nano imprint lithography, molecular dynamics simulations, atomic force microscope, polymer, density

1 INTRODUCTION

Photolithography is widely used to fabricate small patterns. It is, however, expected to be limited due to the diffraction of the light source. Therefore, a number of alternative techniques have been researched to overcome the difficulty fabricating patterns below the the tens of nanometers range.

Among them, novel techniques have emerged with a potential to revolutionize patterning called nano imprint lithography (NIL) by Chou [1], [2]. This technique makes use of the mechanical deformation of a polymer film layer under pressure and temperature. The main advantages in this process compared with other lithography techniques are its low cost, high throughput, no diffraction, and the possibility of large area processing. Despite its advantages, it has proved to have defects that are mechanical in origin.

In this paper, we will focus on the density variations that may take place during the nano imprint lithography process along the patterned structures through experiments and molecular dynamic analysis. Our approach will show a set of rules that, allows us to choose an adequate temperature for the NIL process.

2 EXPERIMENTS

2.1 Thermal Nano Imprint Process

The thermal imprinting processes were performed on an EVG®520HE system using a silicon wafer with spin-coated polymethymeta acrylate (PMMA) as the substrate and under a vacuum of 7×10^{-3} mbar. The 600 nm patterns were imprinted in the 150 ㎜ × 200 ㎜ polyurethane acrylate (PUA) stamp at 140℃, 170℃ and 200℃ while under a force of 500N for 25mins.

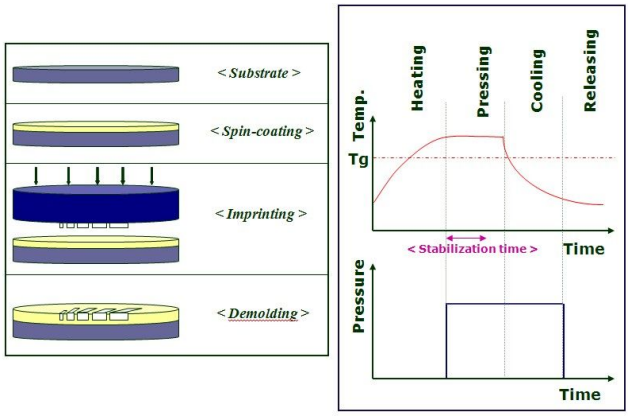

(a) (b)

Fig 1 Thermal NIL process:
(a) NIL process steps, (b) Process diagram

2.2 Experimental Measurement Details

After patterning, we estimated the local density by measuring the pull-off force between the sharp tip and the patterned surface using an atomic force microscope (AFM) in liquid. The measured pull-off forces were averaged to statistical significance over 100-150 locations on each sample surface.

The pull-off adhesion force can be a combination of many forces such as the van der Waals, the capillary, the electrostatic and the chemical forces ($F_{ad} = F_{el} + F_{vdW} + F_{cap} + F_{chem}$). Among these forces, as we performed the measurements in a liquid (Perfluorinated decalin (C10F18)) to reduce the contribution from other forces, the van der Waals interactions was found to be dominant [3].

The adhesion force between an AFM tip and a flat surface in perfluoriated decain of open liquid cell is calculated by the Johnson-Kendall-Roberts relation [4] :

F_{JKR}=-1.5πWR (1)

where R is the effective radius of the AFM tip (~ 10 nm) and W is the work of adhesion between three mediums. The work of adhesion among the tip, the polymer surface and the liquid can be calculated by $W = A_{total}/(12 \times \pi D_0^2)$, where A is the Hamaker constant and D_0 (0.165 nm) is the cutoff length [5]. After inserting $A= 7.11 \times 10^{-20}$ for the PMMA, 6.5×10^{-20} for the silicon oxide tip and 2.14×10^{-20} for Perfluorinated decalin ($C_{10}F_{18}$) [5], [6], respectively. The effective Hamaker constant was calculated to be 1.3078×10^{-20}, therefore, the theoretical van der Waals adhesion force was 0.6005nN, which is in agreement with the experimental data that will be shown in sec. 4. One fundamental postulation here is that the adhesion force is proportional to the density of the resist since the Hamaker constant also increases with an increasing number of atoms per unit area or the density of the film [7].

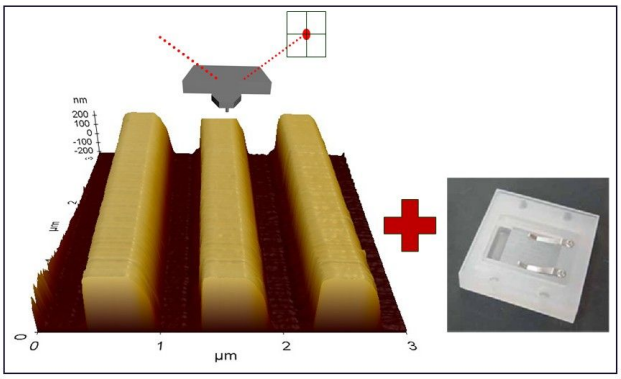

Fig 2 Schematic measurement set up

3 MOLECULAR DYNAMICS SIMULATIONS

In order to compare with the experimental data, we carried out molecular dynamics (MD) simulations.

3.1 Model of NIL System

The model of the NIL system consists of 3 parts: the stamp, the polymer resist and the substrate. This model is similar to the actual NIL process system.

Polymer resist is composed of amorphous polyethylene (PE). There are 75 PE molecules in polymer resist, and the molecular weight of each PE molecule is about 2,802 (degree of polymerization = 100).

The stamp is composed of 19,665 nickel atoms with a FCC structure. The width of the cavity is 5nm and the height is 2nm. The substrate is composed of 5,476 silicon atoms with a diamond cubic structure.

3.2 Force Field of the NIL System

We adopt a beads spring potential model to compute the interactions between the atoms in the PE molecules. In this model, the methyl and ethyl atom groups are considered to be united atoms.

This potential model contains 4 potentials: the bond, the angle, the torsion and the Lennard Jones 12-6 (LJ) potential [8], [9]. For the internal polymer chain, the bond, the angle, the torsion and the LJ potential are used. The LJ potential is applied not only between atoms in polymer chains, but also between atoms in the stamp or the substrate. We use the Lorentz-Berthelot mixing rules to calculate the parameters for two different united atoms. For efficiency, we calculate the LJ potential within the cut-off radius (2.5σ) [8]:

$$\Phi_{bond} = \frac{1}{2} K_{bond} \left(l_{ij} - l_0 \right)^2 \quad (2)$$

$$\Phi_{angle} = \frac{1}{2} K_{angle} \left(\theta_{ijk} - \theta_0 \right)^2 \quad (3)$$

$$\Phi_{torsion} = \sum_{m=0}^{3} a_m \left\{ \cos(\phi_{ijkl}) \right\}^m \quad (4)$$

$$\Phi_{LJ} = 4\varepsilon_{ij} \left\{ \left(\frac{\sigma_{ij}}{r_{ij}} \right)^{12} - \left(\frac{\sigma_{ij}}{r_{ij}} \right)^{6} \right\} \quad (5)$$

3.3 Assumption for Simulation

When we perform the MD simulations, we made the following assumptions: First, the interaction forces between the molecules of the stamp and the substrate are neglected because the interactions between these atoms and polymer chains consist only of repulsive forces. During the MD simulations, we also assume that there is no dissociation and cross-linking in polymer chains and the system is at a quasi-equilibrium state.

3.4 Simulation Procedure

Before the simulation, the polymer resist needed to be well dispersed in order to minimize the potential energy. Over 50,000 dispersion steps were required to reach the minimum potential energy.

In this study, the imprint process is divided into four stages: initial relaxation, imprinting, stabilization and releasing. The temperature is kept constant during the imprinting stage. After cooling, the temperature is held constant again for the releasing stage. We control the temperature of the system with the canonical NVT ensemble method during the simulation and the time integration is performed using a leap frog method.

We performed simulations for 350K, 400K and 450K.

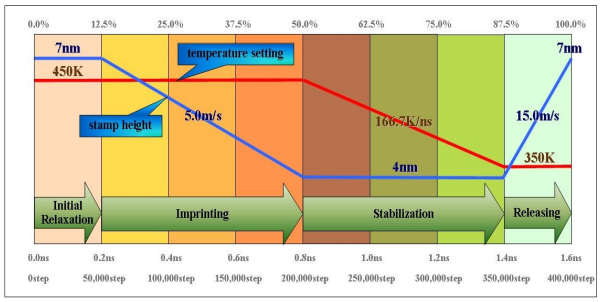

Fig 3 The imprint process cycle in four stages: initial relaxation (0.2ns), imprinting (0.8ns), stabilization(1.4ns) and releasing (1.6ns) [7].

4 RESULTS

4.1 Experimental Results

Figs. 1 and 2 show a schematic diagram of the experimental procedure. The ratio of the pull-off force for the three different temperatures indicates that the density of the top was always less than that of the bottom. The measured pull-off force typically ranged from 0.20 nN to 0.91 nN; it was 0.351nN (±0.25 nN) at the top and 0.397nN (± 0.203 nN) at the bottom for the pattern imprinted at 140℃. Some deviations between the experiment and the theory might be attributed to the non-uniform contact of the tip. Fig 4 shows the top to bottom density ratio that ranged 0.881 for 140℃, 0.905 for 170℃ and 0.966 for 200℃.

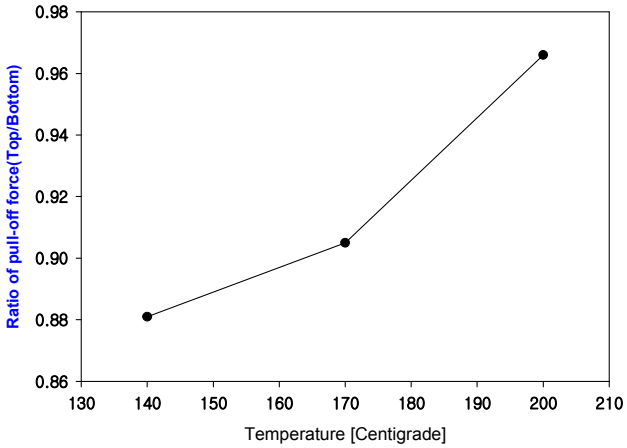

Fig 4 Experimental results

4.2 Simulation Results

Fig 5 shows, that the density ratio from the simulation goes up with the imprinting temperature. The measured density difference ratios were 0.807 for 400K, 0.793 for 350K and 0.787 for 300K.

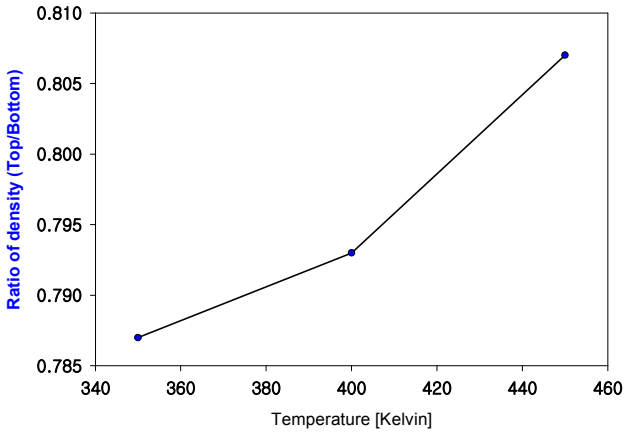

Fig 5 Molecular dynamics simulation results

4.3 Conclusion

We investigated the local density variation of the polymer resist for different imprinting temperatures through both experimentation and simulations. The experimental data and simulations showed a good agreement at least in a qualitative sense. The density difference between the top and the bottom regions was found to decrease as the processing temperature increases.

Acknowledgments

This research was supported by a grant(08K1401-00710) from the Center for Nanoscale Mechatronics & Manufacturing, one of the 21st Century Frontier Research Programs, which are supported by the Ministry of Education, Science and Technology, KOREA

REFERENCES

[1] CHOU, S. Y., KRAUSS, P. R. & RENSTROM, P. J. (1995) Imprint of sub-25 nm vias and trenches in polymers. *Applied Physics Letters*, 67, 3114.
[2] CHOU, S. Y., KRAUSS, P. R. & RENSTROM, P. J. (1996) Imprint Lithography with 25-Nanometer Resolution. *Science*, 272, 85.
[3] BUTT, H. J., CAPPELLA, B. & KAPPL, M. (2005) Force measurements with the atomic force microscope: Technique, interpretation and applications. *Surface Science Reports*, 59, 1-152.
[4] JOHNSON, K. L., KENDALL, K. & ROBERTS, A. D. (1971) Surface Energy and the Contact of Elastic Solids. *Proceedings of the Royal Society of London. Series A, Mathematical and Physical Sciences (1934-1990)*, 324, 301-313.

[5] ISRAELACHVILI, J. N. (1991) *Intermolecular and surface forces*, London, Academic Press.
[6] BERGSTROM, L. (1997) Hamaker constants of inorganic materials. *Advances in Colloid and Interface Science*, 70, 125-169.
[7] WOO, Y. S., KIM, J. K., LEE, D. E., SUH, K. Y. & LEE, W. I. (2007) Density variation of nanoscale patterns in thermal nanoimprint lithography. *Applied Physics Letters*, 91, 253111.
[8] KOYAMA, A., YAMAMOTO, T., FUKAO, K. & MIYAMOTO, Y. (2001) Molecular dynamics studies on local ordering in amorphous polyethylene. *The Journal of Chemical Physics*, 115, 560.
[9] YASHIRO, K., ITO, T. & TOMITA, Y. (2003) Molecular dynamics simulation of deformation behavior in amorphous polymer: nucleation of chain entanglements and network structure under uniaxial tension. *International Journal of Mechanical Sciences*, 45, 1863-1876.